Palladium complexes containing bis(oxazolines): stoichiometric *versus* catalytic allylic alkylation

Montserrat Gómez,*[a] Susanna Jansat,[a] Guillermo Muller,*[a] Miguel A. Maestro,[b] José Mahía Saavedra,[b] Mercè Font-Bardía[c] and Xavier Solans[c]

[a] *Departament de Química Inorgànica, Universitat de Barcelona, Martí i Franquès 1-11, E-08028 Barcelona, Spain*
[b] *Edificio anexo Facultade de Ciencias, Servicios Xerais de Apoio á Investigación, Campus da Zapateira, s/n, Universidade da Coruña, E-15071 A Coruña, Spain*
[c] *Departament de Cristal.lografia, Mineralogia i Dipòsits Minerals, Universitat de Barcelona, Martí i Franquès s/n, E-08028 Barcelona, Spain*

The allylic palladium complexes (**1L**, for allyl = η^3-C$_3$H$_5$; **2L**, for allyl = η^3-1,3-Ph$_2$C$_3$H$_3$) with chiral 1,2-bis-(oxazolinyl)benzene and 1,2-bis(oxazolinyl)ethane ligands **L**, (*R,R*)-**A**, (*R,S*)-**A**, (*S,S*)-**B**, (*R,R*)-**C**, and (*S,S*)-**D**, were synthesized and fully characterized, both in solution and in the solid state. Five crystal structures of palladium allyl complexes are described, three of them containing the non-substituted allyl group, (*R,S*)-**1A**, (*S,S*)-**1B**, and (*S,S*)-**1D**, and two containing the 1,3-diphenylallyl group, (*R,S*)-**2A** and (*S,S*)-**2B**. A NMR study showed the existence of two isomers in solution for complexes containing 1,2-bis(oxazolinyl)benzene, *endo* and *exo*, with the diasteromeric excess of *ca.* 40% for type **1** complexes and *ca.* 75% for type **2** complexes. The catalytic behaviour of the palladium systems with the ligands described was tested for a model allylic alkylation reaction. The Pd/bis(oxazolinyl)benzene ((*R,R*)-**A**, (*S,S*)-**B**) catalytic systems showed low activity, but good asymmetric inductions, affording enantiomeric excesses up to 86%. However, the Pd/bis(oxazolinyl)ethane systems exhibited lower activity and worse enantioselectivity than for the analogous catalysts containing the rigid phenyl backbone. Stoichiometric reactions, modelling the nucleophilic attack step of the catalytic cycle, from palladium(II) (**2L**) complexes, led to lower enantiomeric excesses than under catalytic conditions.

Introduction

Although C_2-symmetrical bis(oxazolines) have extensively been used as chiral auxiliary ligands in many metal-catalyzed processes,[1] few of them have been reported in connection with Pd-catalyzed allylic substitution reactions. The ligands tested in these organic processes are those derived from oxalic, malonic, and dimethylmalonic acids.[2] The resulting catalytic palladium systems lead to high enantioselectivity in the model allylic alkylation reaction, reaching 77% ee (enantiomeric excess) for the oxalic derivatives[2a] and 97% for the oxazolines derived from malonic acids.[2c] Upon coordination the latter ligands form a six-membered metal chelate, where the substituents on the oxazoline ring are closer to the metal than in the case of the five-membered rings from bis(oxazolinyl) oxalic ligands. This sterochemical feature and the symmetry of the ligand and the allyl group explain the excellent enantioselectivity found. Consequently, palladium intermediates must be characterised to understand the course of the catalytic reaction. Several NMR studies of allylic palladium complexes containing either bis- or mono-oxazolines have been reported,[2c,3] but only two crystal structures are collected in the Cambridge Structural Data base, concerning palladium complexes with 1,3-diphenylallyl and bis(oxazoline) ligands,[4] derived from dimethylmalonic acid.

To the best of our knowledge, no studies about allylic substitutions with bis(oxazolines) containing more than one carbon spacer between the two heterocycles have been reported. In particular, the 1,2-bis(oxazolinyl)benzene derivatives, introduced by Bolm and co-workers in 1991,[5] gave poor asymmetric inductions in several catalytic processes.[6] The lack of data prompted us to study the catalytic behaviour of chiral two-carbon spacer ligands, rigid and flexible, 1,2-bis(4-R-Δ²-1,3-oxazolin-2-yl)-
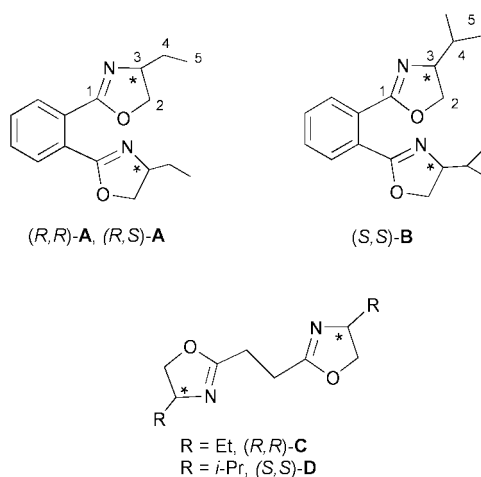

**Fig. 1** Bis(oxazoline) ligands and labeling of the atoms for NMR data.

benzene ligands (R = Et **A** or Pr^i **B**) and 1,2-bis(4-R-Δ²-1,3-oxazolin-2-yl)ethane ligands (R = Et **C** or Pr^i **D**), respectively (see Fig. 1). In order to understand the catalytic results, the synthesis and characterization, both in solution and in the solid state, of the palladium precursors and intermediates are detailed.

Structural characterization

Ligands

The ligands (*R,R*)-**A**, (*R,S*)-**A**, (*S,S*)-**B**, (*R,R*)-**C**, and (*S,S*)-**D**

DOI: 10.1039/b007743g

were prepared following standard methods with minor modifications (see Experimental section).[7] As described previously by us,[7a] ligand **A** is obtained as a mixture of two diastereomers, (*R*,*R*)-**A** and (*R*,*S*)-**A** which could be separated by reaction with nickel perchlorate and further decoordination with potassium cyanide (see Scheme 1). In order to obtain pure (*R*,*R*)-**A**, several

80% (*R*,*R*)-**A** + 20% (*R*,*S*)-**A**
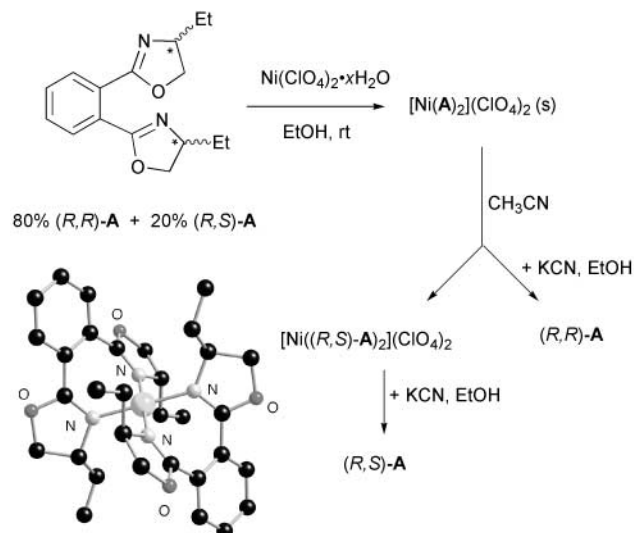
Scheme 1 Separation of diastereomers (*R*,*R*)-**A** and (*R*,*S*)-**A** by nickel complexation. View of the molecular structure of [Ni((*R*,*S*)-**A**)₂][ClO₄]₂. Hydrogen atoms and perchlorate anions are omitted for clarity.

decoordination–coordination cycles from acetonitrile solution were needed. Suitable monocrystals were isolated for complex [Ni((*R*,*S*)-**A**)₂][ClO₄]₂ because of its low solubility under these conditions. As shown in the structure (see Scheme 1), the nickel atom has a square-planar arrangement, coordinated to four nitrogen atoms. The two (*R*,*S*)-**A** ligands are in *trans* position, relative to the bridging phenyl groups between the two oxazoline moieties.

Allylic palladium complexes, 1L and 2L

The allylic palladium complexes containing as ancillary ligands the bis(oxazolines) **A**, **B**, **C**, and **D** (see Scheme 2) were obtained following the general method described in the literature with some modifications (see Experimental section).[8] The complexes

with **A**, **B** were obtained as a mixture of two isomers, *exo* and *endo*, depending on the relative position of the central allylic hydrogen atom and the phenyl bridge of the bis(oxazoline) ligand: *exo* isomer, if both groups point in the same direction; *endo* isomer, if one of them points away from the other group. An important aspect to note is the diastereoselectivity in the synthesis of these allylic complexes. While type **1** complexes show an isomer ratio of *ca.* 70 : 30, those containing the diphenyl allylic group reach a ratio of *ca.* 88 : 12 (except for (*R*,*S*)-**2A**), determined by NMR spectroscopy (see below, NMR discussion). Because of the flexible bridge between the oxazoline moieties, no diastereomers are distinguished in solution in the case of complexes containing ligands **C** and **D**.

Three crystal structures containing the non-substituted allyl group, (*R*,*S*)-**1A**, (*S*,*S*)-**1B**, and (*S*,*S*)-**1D**, and two containing the diphenyl allyl group, (*R*,*S*)-**2A** and (*S*,*S*)-**2B**, could be determined. All of them evidence the loss of the C_2 symmetry of the ligand upon coordination with the metal fragment, as observed for other kinds of complexes with bis(oxazolines).[1] In each of these structures the palladium atom shows a distorted square-planar coordination, bonded to two nitrogen and two terminal allylic carbon atoms. The bond distances and angles around the metal center are in the range observed for other similar complexes.[2] The bite angles, N(1)–Pd–N(2), are less than 90°, except for (*S*,*S*)-**1D** (see Fig. 2), which is exactly 90° (see Table 1), due to the flexibility of the metallic cycle, compared with the phenyl rigid backbones for the structures
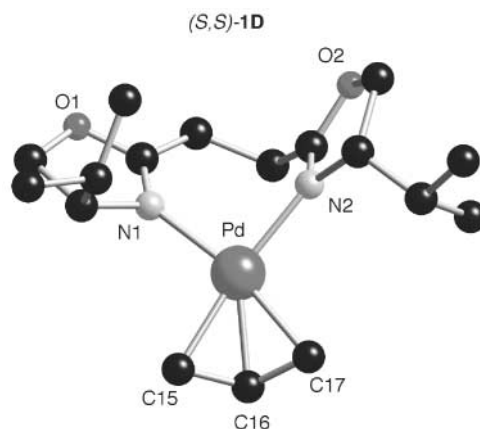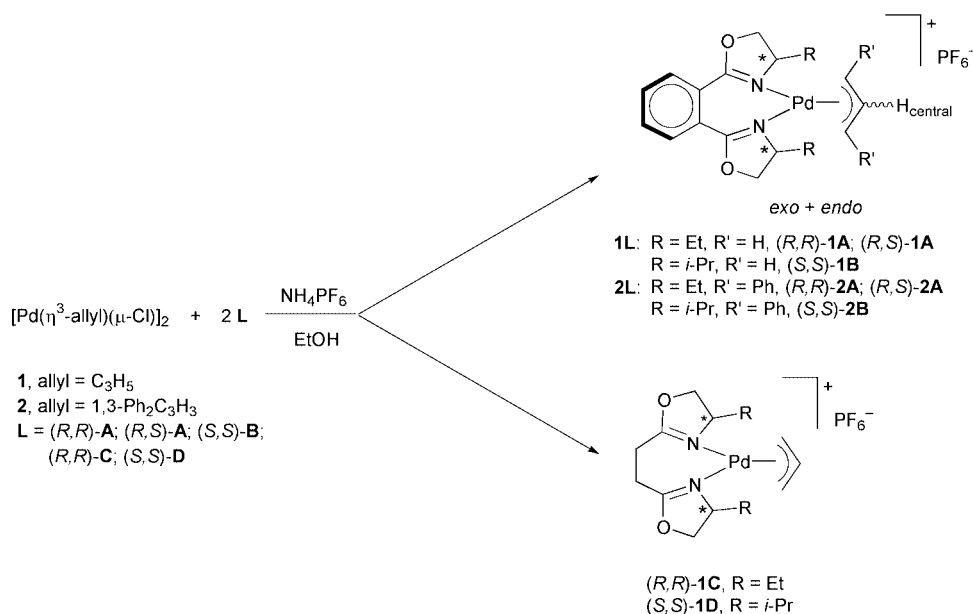

Fig. 2 View of the molecular structure of complex (*S*,*S*)-**1D**. Hydrogen atoms and the hexafluorophosphate anion are omitted for clarity.
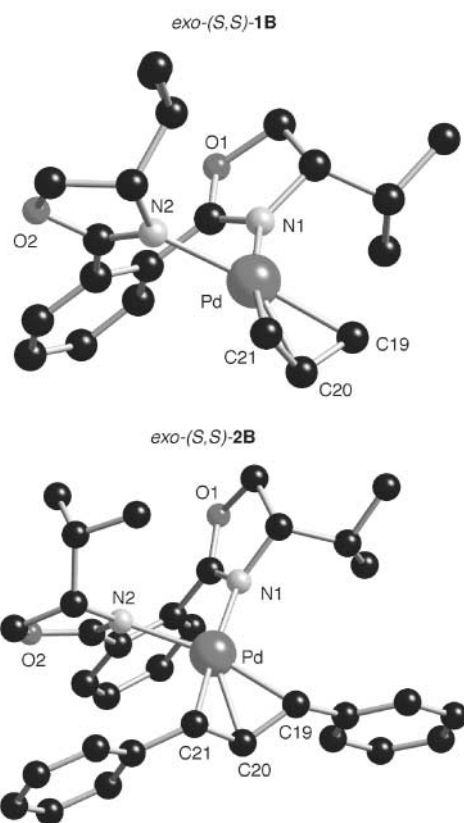

Scheme 2

exo-(S,S)-**1B**

exo-(S,S)-**2B**

Fig. 3 View of the molecular structures of complexes (S,S)-**1B** and (S,S)-**2B**. Details as in Fig. 2.

containing **A** and **B** ligands. Consequently, the isopropyl group is less close to the allyl fragment than in the case of the complexes containing the bis(oxazoline) ligands **A** or **B**. The X-ray analysis of allylic complexes with **A** and **B** ligands revealed which kind of isomer crystallizes in the solid state. Interestingly, only the *exo* isomer crystallizes for complexes (S,S)-**1B** and (S,S)-**2B**, whereas *exo* and *endo* conformations are obtained for (R,S)-**1A** and (R,S)-**2A**, respectively. For the structures derived from the (S,S)-**B** ligand (see Fig. 3) relevant differences are observed concerning the Pd–C$_{terminal\ allyl}$ bond lengths (see Table 1). While for (S,S)-**1B** both distances are very similar (Pd–C19 2.118 (4) Å and Pd–C21 2.111 (4) Å), for (S,S)-**2B** the difference is more important (2.148 (4) and 2.134 (4) Å). In the latter complex the longer Pd–C bond length corresponds to the carbon atom that shows more hindrance because of the proximity of the isopropyl group of the oxazoline moiety to the allylic phenyl group. Similar structural behaviour was observed by Pfaltz and co-workers with bis(oxazolines) derived from dimethylmalonic acid.[2e] In contrast, for the structures containing the *meso* ligand (R,S)-**A** (see Fig. 4), the palladium–terminal allylic carbon distances are very similar to each other, for each complex (Pd–C(17) and Pd–C(19), see Table 1). In particular for (R,S)-**2A** the ethyl groups of the oxazoline fragments are far away from the allyl group and no steric strain is produced, as both point to the metallic environment.

The carbon–carbon distances for the allyl fragment are also worthy of note. Using C_2 symmetrical ligands (S,S)-**B** or (S,S)-**D** either for complexes **1** or **2**, the C$_{central}$–C$_{terminal}$ bond corresponding to the terminal carbon close to the isopropyl group is longer than the other one (see Table 1, C–C distances concerning C15 to C21). The difference (C(15)-C(16) *vs.* C(16)-C(17)) is 0.018 Å for (S,S)-**1D**, but for (S,S)-**1B** it is 0.032 Å and for (S,S)-**2B**, 0.026 Å (in these structures, comparing the distances C(19)-C(20) and C(20)-C(21)). These data show the relationship between the electronic distribution and the steric interaction of the oxazolinic substituent with the allyl group. When the *meso* ligand is involved the difference between
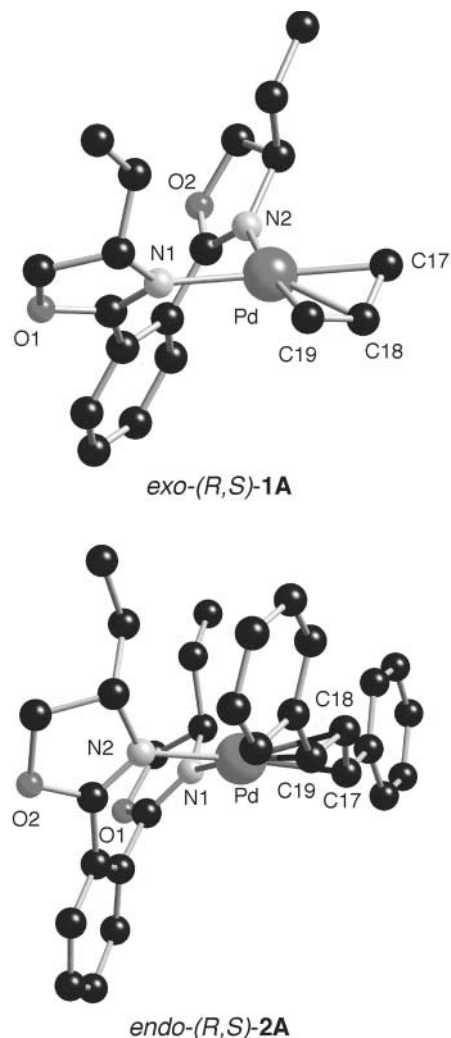
exo-(R,S)-**1A**

endo-(R,S)-**2A**

Fig. 4 View of the molecular structures of complexes (R,S)-**1A** and (R,S)-**2A**. Details as in Fig. 2.

both C–C lengths (in this case, C(17)-C(18) and C(18)-C(19)) is less important, reaching 0.018 Å for (R,S)-**2A**, analogous to (S,S)-**1D**.

The structure in solution of all the allylic complexes was determined by NMR spectroscopy. Only the (R,R)-**1A** complex showed broad signals in the range of temperatures studied (223–330 K). Owing to the loss of C_2 symmetry of the ligands upon coordination, the two oxazoline fragments are not equivalent and therefore the *anti* and *syn* allyl protons each exhibit different chemical shifts (see Table 2).

When ethenyl bridge chiral ligands were used a C_2 symmetry could be assumed for the coordinated bis(oxazoline) in which case isomers are not distinguished are possible for [Pd(η³-C₃H₅)(**L**)] where **L** = **C** or **D**. Their 2-D NOESY spectra enable the allyl and oxazolinyl fragments to be correlated by NOE contacts. In addition, the exchange signals between protons of both oxazoline groups indicate rotation around the allyl–palladium bond.

Either type **1** or **2** complexes, containing 1,2-bis(4-R-Δ²-1,3-oxazolin-2-yl)benzene ligands, were obtained as a mixture of two isomers. Their ratio did not change with temperature, as shown by ¹H NMR spectra measured in the 223–330 K range. The ¹H NMR spectra of single crystals obtained for the X-ray analysis (see above) led to the elucidation of the *exo* and *endo* isomers in solution, in each case. Consistent with the solid structural data, for complexes containing the (S,S)-**B** ligand, the *major* isomer corresponds to the *exo* one, and for those containing the (R,S)-**A** ligand the *major* species shows an *exo* conformation for (R,S)-**1A** and *endo* for (R,S)-**2A**. 2-D

Table 1 Selected bond lengths (Å) and bond angles (°) for (R,S)-1A, (R,S)-2A, (S,S)-1B, (S,S)-2B, and (S,S)-1D (with esds in parentheses)

	(R,S)-1A	(R,S)-2A	(S,S)-1B	(S,S)-2B	(S,S)-1D
Pd–N(1)	2.061(3)	2.104(4)	2.096(3)	2.110(4)	2.118(7)
Pd–N(2)	2.067(3)	2.105(4)	2.096(3)	2.113(3)	2.097(7)
Pd–C(15)	—	—	—	—	2.122(10)
Pd–C(16)	—	—	—	—	2.094(6)
Pd–C(17)	2.127(5)	2.154(5)	—	—	2.121(9)
Pd–C(18)	2.111(5)	2.135(4)	—	—	—
Pd–C(19)	2.120(5)	2.153(4)	2.118(4)	2.148(4)	—
Pd–C(20)	—	—	2.110(4)	2.117(4)	—
Pd–C(21)	—	—	2.111(4)	2.134(4)	—
C(15)–C(16)	—	—	—	—	1.385(14)
C(16)–C(17)	—	—	—	—	1.403(13)
C(17)–C(18)	1.358(7)	1.413(7)	—	—	—
C(18)–C(19)	1.348(7)	1.395(7)	—	—	—
C(19)–C(20)	—	—	1.404(6)	1.421(5)	—
C(20)–C(21)	—	—	1.372(7)	1.395(5)	—
N(1)–Pd–N(2)	86.99(11)	87.08(14)	86.20(13)	85.51(14)	90.0(3)
C(15)–Pd–C(17)	—	—	—	—	69.3(4)
C(17)–Pd–C(19)	70.0(2)	68.13(18)	—	—	—
C(19)–Pd–C(21)	—	—	69.0(2)	68.7(2)	—
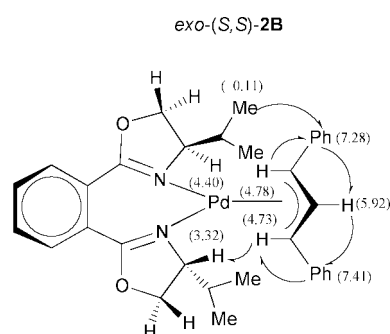
Fig. 5 Selected NOE contacts (indicated by arrows) for exo-(S,S)-2B, showing the correlation between the diphenylallyl and the oxazoline fragments. Chemical shifts are in parentheses.

NOESY experiments were especially useful because they allowed us to assign all the protons for each isomer (exo and endo). For instance Fig. 5 contains the NOE contacts between the two non-equivalent oxazolines and the diphenylallyl fragment for exo-(S,S)-2B, showing clearly the electronic effect of the phenyl ring over one of the isopropyl substituents (one of the methyl groups appears at high field, δ −0.11).

In addition, exchange signals between both isomers, between oxazolinic or allylic protons, were observed for both kinds of complexes, 1L and 2L. This, along with the temperature behaviour in solution, shows that the exo and endo isomers are in equilibrium, but with a low interconversion rate. In order to determine this, an NMR experiment using two-site magnetiz-ation transfer[9] was also done for (R,S)-2A, irradiating selec-tively the central allylic protons and the methyl groups for each isomer. In all events, the non-irradiated signal did not change in intensity, which means that the interconversion rate between exo and endo isomers cannot be quantified on the NMR time-scale. Interestingly, for type 2 complexes, the central allylic proton atoms for the exo isomers always appear at high field relative to the endo complexes, whereas the chemical shifts of the central allylic carbon show the opposite trend (see Table 2). In addition, both terminal allylic carbon atoms have the same carbon chemical shifts for (R,S)-2A, which corroborates the similar Pd–C bond distances observed in the solid state (see above). However for the other complexes, these atoms are not equivalent, showing a higher difference between them, for the endo than for the exo complexes (ca. 3 versus 1 ppm, respec-tively). Since both terminal allylic positions are distinguished by the steric hindrance between the oxazoline and the allylic phenyl groups, we can conclude that the endo isomers contain-

ing (R,R)-A and (S,S)-B are less stable than the exo ones. These latter complexes are the main species in solution.

To corroborate these experimental data, semi-empirical calculations (PM3(tm) level) were carried out for (R,R)-2A and (S,S)-2B, in each case for exo and endo configurations. For both systems the exo isomer showed a lower formation enthalpy than that of the endo one.
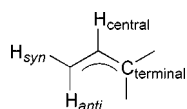
Catalytic and stoichiometric reactions

The palladium/bis(oxazoline) systems described here were tested in model allylic alkylation, between the racemic substrate rac-3-acetoxy-1,3-diphenyl-1-propene and dimethyl malonate, under basic Trost conditions.[10] The catalytic results are sum-marized in Table 3. The catalyses were run in situ (1 mol% [Pd(η³-C₃H₅)(μ-Cl)]₂ and 2.5 mol% L) and using allylic pre-cursors (complexes 1L). In both cases the results were similar, in conversion and selectivity. When the complex (S,S)-2B was used as catalytic precursor no change in enantioselectivity was observed, but the conversion was lower than with the catalytic complex (S,S)-1B (65% conversion of substrate after one week, under the conditions described in Table 3).

The ligands (R,R)-A and (S,S)-B gave good enantioselectiv-ity, up to 86% enantiomeric excess, but low activities, achieving total consumption of starting allylic acetate after 36–80 h (entries 2 and 3 of Table 3). The meso ligand (R,S)-A afforded a very low asymmetric induction (entry 1), according to the not-able symmetry of the allyl group for the intermediate (R,S)-2A, in solution and in the solid state (see above). The Pd/ bis(oxazolinyl)ethane systems also gave very low activity and selectivity (entries 4 and 5), with Pd/(S,S)-D the results were better than with Pd/(R,R)-C because the isopropyl hindered more than the ethyl substituent, as observed between (R,R)-A and (S,S)-B.

It is generally accepted that the enantioselectivity of the overall process is determined by the regioselectivity of nucleophilic attack at the terminal carbon allylic position in the allylic palladium(II) intermediate. Comparison between the diastereomeric excesses (des) of type 2 complexes and the enantiomeric excesses of the catalytic reaction showed a good match between the two pieces of data, although the des are lower than the ees, mainly in the (S,S)-B system. Then, in order to corroborate the source of the enantioselectivity, we carried out stoichiometric alkylations by reaction of type 2 complexes and the nucleophile (see eqn. (1)), under similar basic conditions to those described before for the catalytic process. This reaction was very fast, being complete after

Table 2 Selected ^{1}H (CDCl$_3$, δ in ppm, 500 MHz, 298 K) and ^{13}C (CDCl$_3$, δ in ppm, 63 MHz, 298 K) NMR data ^{a} for allylic complexes containing ligands (R,R)-**A**, (R,S)-**A**, (S,S)-**B**, (R,R)-**C**, and (S,S)-**D**

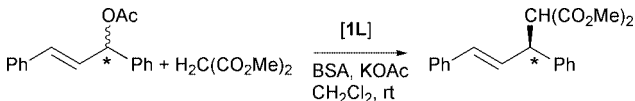| Complex	H²ᵇ	H³	H⁴	H⁵	H_syn	H_anti-[C_terminal]	H_central-[C_central]
(R,S)-1Aᶜ							
exo (73%)	4.32 (5, 2H, 8.0) 4.84 (dd, 2H, 10, ᵈ	4.42 (m, 2H)	1.71 (m, 4H) 2.13 (m, 4H)	1.03 (t, 6H, 7.5)	4.02 (d, 2H, 6.5)	2.91 (d, 2H, 12.5)	5.27 (m, 1H)
endo (27%)		4.35 (m, 2H)	1.54 (m, 2H) 1.90 (m, 2H)	0.96 (t, 6H, 7.25)	4.05 (d, 2H, 7.5)	2.86 (d, 2H, 12.5)	5.65 (m, 1H)
(S,S)-1Bᵉ							
exo (71%)	4.54 (bdd, 2H, 10.0, 2.5) 4.40 (bt, 2H, 6.5)	4.80 (m)ᶠ	2.28 (m, 2H)	0.83 (d, 3H, 7.0) 1.02 (m, 9H)	3.80 (dd, 1H, 7.0, 1.5) 4.24 (dd, 1H, 7.0, 1.5)	2.96 (d, 1H, 12.5) 3.06 (d, 1H, 12.5)	5.31 (ph, 1H)
endo (29%)	4.34 (m, 1H) 4.42 (m, 1H) 4.47 (bdd, 1H 8.0, 4.0) 4.51 (m, 1H)	4.80 (m)ᶠ	2.05 (m, 1H) 2.18 (m, 1H)	0.86 (b)ᵍ 0.89 (d, 3H, 6.5) 0.94 (d, 3H, 7.0) 1.00 (b)ᵍ	4.00 (bd, 1H, 6.5) 4.16 (bd, 1H, 6.5)	2.76 (d, 1H, 12.5) 2.95 (d, 1H, 12.5)	5.60 (ph, 1H)
(R,S)-2A							
endo (67%)	3.98 (dd, 2H, 9.0, 7.0) 4.26 (t, 2H, 9.0)	2.41 (m, 2H)	1.15 (m, 2H) 1.66 (m, 2H)ᵈ	0.58 (t, 6H, 7.0)	—	4.70 (d, 2H, 12.0) [76.8]	6.70 (t, 1H, 12.0) [105.3]
exo (33%)	4.05 (d, 4H, 9.0)	3.39 (m, 2H)	1.66 (m, 2H)ᵈ 2.11 (m, 2H)	0.99 (t, 6H, 7.5)	—	4.72 (d, 2H, 11.5) [77.0]	6.07 (t, 1H, 11.5) [108.1]
(R,R)-2A							
exo (89%)	3.73 (dd, 1H, 10.0, 9.0) 3.96 (t, 1H, 9.0) 4.05 (dd, 1H, 9.0, 7.0) 4.56 (dd, 1H,	3.39 (m, 1H) 4.33 (m, 1H)	0.76 (m, 1H) 1.67 (m, 2H)ᵈ 1.82 (m, 1H)	0.57 (t, 3H, 7.5) 0.96 (t, 3H, 7.5)	—	4.68 (d, 1H, 11.5) 4.69 (d, 1H, 11.5) [78.0, 77.3]	5.91 (t, 1H, 11.5) [109.9]
endo (12%)	4.17 (dd, 1H, 9, 8.5) 4.26 (dd, 1H, 9, 8.5) 4.47 (bt, 1H, 10.5) 4.52 (bt, 1H,	3.83 (m, 1H) 4.05 (m, 1H)	0.21 (m, 1H) 1.67 (m, 2H)ᵈ 1.89 (m, 1H)	0.48 (t, 3H, 7.5) 0.67 (t, 3H, 7.5)	—	4.72 (d, 1H, 12.0) 4.81 (d, 1H, 12.0) [80.9, 77.7]	6.54 (t, 1H, 12.0) [105.4]
(S,S)-2B							
exo (87%)	3.60 (bt, 1H, 9.5) 4.08 (dd, 1H, 9.0, 6.0) 4.25 (dd, 1H, 9.0, 6.0) 4.33 (bt, 1H, 9.5)	3.32 (m, 1H) 4.40 (m, 1H)	1.65 (m, 1H) 2.18 (m, 1H)	−0.11 (d, 3H, 6.5) 0.88 (d, 3H, 7.0) 0.90 (d, 3H, 7.0) 0.93 (d, 3H, 7.0)	—	4.73 (d, 1H, 11.5) 4.78 (d, 1H, 11.5) [78.0, 77.1]	5.92 (t, 1H, 11.5) [109.4]
endo (13%)	4.02 (bt, 1H, 9.0) n.d.ʰ	3.86 (m, 1H) n.d.ʰ	1.74 (m, 1H) 2.25 (m, 1H)	0.27 (d, 3H, 6.5) 0.53 (d, 3H, 7.0) 0.62 (d, 3H, 7.0) 0.66 (d, 3H, 7.0)	—	4.58 (d, 1H, 11.5) n.d.ⁱ [79.6, 75.5]	6.52 (t, 1H, 11.5) [105.3]
(R,R)-1Cʲ	4.16 (m, 2H) 4.53 (pt, 1H, 9.5) 4.58 (pt, 1H, 9.0)	4.02 (m, 1H) 4.08 (m, 1H)	1.55 (m, 1H) 1.68 (m, 1H) 1.76 (m, 1H) 1.86 (m, 1H)	0.86 (t, 3H, 7.5) 0.92 (t, 3H, 7.5)	4.02 (pdd, 1H, 1.75, 6.75) 4.15 (pdd, 1H, 2.5, 6.75)	3.00 (d, 1H, 12.5) 3.08 (d, 1H, 12.5)	5.63 (m, 1H)
(S,S)-1Dᵏ	4.25 (m, 2H) 4.41 (m, 2H)	4.00 (m, 1H) 4.06 (m, 1H)	2.07 (m, 1H) 2.17 (m, 1H)	0.77 (d, 3H, 7.0) 0.85 (d, 3H, 7.0) 0.92 (d, 3H, 7.0) 0.95 (d, 3H, 7.0)	4.00 (dd, 1H, 2.0, 7.0) 4.18 (dd, 1H, 2.5, 7.0)	3.01 (d, 1H, 12.5) 3.12 (d, 1H, 12.5)	5.65 (m, 1H)

^{a} Multiplicity (b, broad; d, doublet; h, heptuplet; m, multiplet; p, pseudo; q, quartet; s, singlet; t, triplet), relative integration, and coupling constants (in Hz) in parentheses. In square brackets, the ^{13}C chemical shifts. ^{b} See Fig. 1 for atom labeling. ^{c} Spectrum measured at 278 K. ^{d} Protons of the minor isomer overlapped with those of the major isomer. ^{e} Spectrum measured at 273 K. ^{f} H³ signals for exo and endo isomers overlapped. ^{g} Overlapped by methyl signals of the major isomer. ^{h} Not distinguished; signals overlapped by other major isomer signals. ^{i} Not distinguished; by NOESY experiment, this anti proton is below the anti protons of the major isomer. ^{j} Methylenic backbone chemical shifts: δ 2.76 (m, 2H) and 2.96 (m, 2H). ^{k} Methylenic backbone chemical shifts: δ 2.76 (m, 1H), 2.85 (m, 1H), 3.00 (m, 1H), 3.10 (m, 1H).

15–20 minutes at room temperature. Surprisingly, the enantiomeric excess of the product was, in all cases, very low (up to 36% for (S,S)-**2B** complex, see eqn. (1)). These results suggest that the enantioselectivity could also be controlled by the oxidative addition step of the allylic acetate over the catalytically active palladium(0) species, prior to the

Table 3 Results of asymmetric allylic alkylation of *rac*-3-acetoxy-1,3-diphenyl-1-propene with dimethyl malonate[a]

Entry	Precursor	Time/h	Conversion (%)[b]	ee (%)[c]	Configuration[d]
1	(*R,S*)-**1A**	36	100	10	*R*
2	(*R,R*)-**1A**	36	100	78	*R*
3	(*S,S*)-**1B**	80	95	86	*S*
4	(*R,R*)-**1C**	168	100	7	*R*
5	(*S,S*)-**1D**	168	95	23	*S*

[a] Results determined from duplicate experiments. [b] Based on the substrate, determined by ¹H NMR spectroscopy. [c] Determined by HPLC on a Chiralcel-OD column. [d] Determined by optical rotation.[11]

(1)
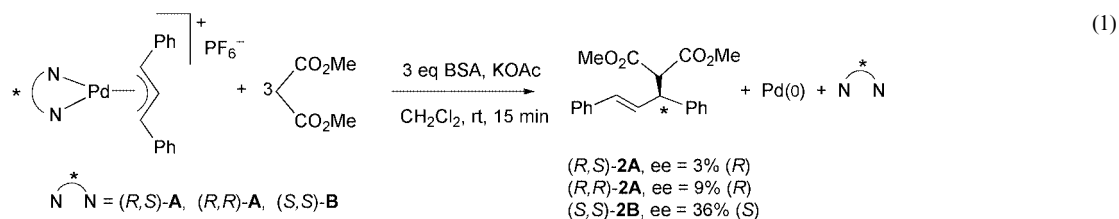
nucleophilic attack, which was the slowest step in the overall process.

Conclusion

When the bis(oxazoline) ligands studied here coordinate with palladium seven-membered metallocycles, which differ in their flexibility, are formed. While for ligands **A** and **B** the two oxazoline groups are connected by two C_{sp2} ("phenyl bridge"), for **C** and **D** two C_{sp3} ("CH_2CH_2 bridge") separate the fragments. This topological feature means the existence of two geometrical isomers, *exo* and *endo*, for allylic complexes **1A**, **1B**, **2A**, and **2B**, due to the relative position of the allyl and the phenyl bridge groups. The structural studies, in solid state and in solution, indicate that the *exo* conformations are more stable for (*R,R*)-**A** and (*S,S*)-**B** than the *endo* ones.

The allylic systems, **1L**, were tested in a model catalytic allylic alkylation. Although the complexes containing (*R,R*)-**C** and (*S,S*)-**D** ligands only show one isomer in solution, the enantiomeric excesses in the allylic alkylation are lower than for catalytic systems containing (*R,R*)-**A** or (*S,S*)-**B**. The more rigid backbone for these latter ligands leads to greater differentiation between the two terminal allylic carbon atoms, due to the higher steric hindrance between the allyl and the substituent on the stereocentre, than for **C** and **D**.

The low asymmetric induction observed in stoichiometric allylic alkylation prompts us to do further investigations with palladium(0) species, which are currently in progress.

Experimental

General data

All compounds were prepared under a purified nitrogen atmosphere using standard Schlenk and vacuum-line techniques. $ZnCl_2$ (Merck) and the solvents were purified by standard procedures and distilled under nitrogen.[12] L-(−)-2-Aminobutanol (Janssen) was used without previous purification. L-Valinol,[13] ligands **A**,[7a] **D**,[5] [Pd(η³-C₃H₅)(μ-Cl)]₂,[14] and [Pd(η³-1,3-Ph₂C₃-H₃)(μ-Cl)]₂[2c] were prepared as described previously. NMR spectra were recorded on Varian XL-500 (¹H, standard SiMe₄), Gemini (¹H, 200 MHz, standard SiMe₄), and Bruker DRX 250 (¹³C, 63 MHz, standard SiMe₄) spectrometers. Chemical shifts are reported downfield from standards. IR spectra were recorded on a Nicolet 520 FT-IR spectrometer. FAB mass chromatograms were obtained on a Fisons V6-Quattro instru-

ment. The GC analysis, for chiral ligands, was performed on a Hewlett-Packard 5890 Series II gas chromatograph (25 m FS-cyclodex-β-I/P column) with a flame ionization detector. Enantiomeric excesses were determined by HPLC on a Hewlett-Packard Series 1050 chromatograph (Chiralcel-OD chiral column) with a UV detector. Optical rotations were measured on a Perkin-Elmer 241MC spectropolarimeter. Elemental analyses were carried out by the Serveis Científico-Tècnics of the University of Barcelona in an Eager 1108 microanalyzer.

Preparations

1,2-Bis[(4*S*)-(4-isopropyl-Δ²-1,3-oxazolin-2-yl)]benzene, (*S,S*)-B.[5] L-Valinol (3.63 cm³, 32.8 mmol), *o*-dicyanobenzene (1.05 g, 8.20 mmol), and anhydrous $ZnCl_2$ (50 mg, 0.04 mmol) were dissolved in 35 cm³ of toluene and refluxed under nitrogen for four days, until no nitrile was observed (reaction monitored by gas chromatography). The reaction mixture was filtered, washed with water, and the organic phase dried over anhydrous Na_2SO_4. The solvent was removed under vacuum, affording a pale yellow oil. The product was purified by SiO_2 column chromatography (ethyl acetate–hexane, 2 : 1, with 2% triethylamine). Yield: 2.26 g (92%). $[a]_D^{25} = -53.5$ deg cm³ g⁻¹ dm⁻¹ (*c* 1.7 g cm⁻³, CHCl₃).

1,2-Bis[(4*R*)-(4-ethyl-Δ²-1,3-oxazolin-2-yl)]ethane, (*R,R*)-C.[5] 0.80 g (10 mmol) of succinonitrile, 4.45 cm³ (50 mmol) of L-(−)-2-aminobutanol, and 0.068 g (0.5 mmol) of anhydrous $ZnCl_2$ were dissolved in 30 cm³ of toluene and refluxed for five days, until the starting nitrile had been consumed (monitored by gas chromatography). The reaction mixture was filtered, washed with water, and the organic phase dried over anhydrous Na_2SO_4. The solvent was removed under vacuum, affording a pale yellow oil. The product was purified by SiO_2 column chromatography (ethyl acetate–hexane, 1 : 3). Yield: 1.57 g (70%). ¹H NMR data (200 MHz, CDCl₃): δ 0.81 (t, *J* 7.4, 6H); 1.40 (m, 4H); 2.50 (s, 4H); 3.74 (pt, *J* 7.6, 2H); 3.90 (m, 2H); 4.20 (pt, *J* 8.6 Hz, 2H). ¹³C NMR data (63 MHz, CDCl₃): δ 9.5 (CH₃); 23.6 (CH₂); 27.4 (CH₂); 66.3 (CH); 70.9 (CH₂); 164.9 (C).

(η³-Allyl){1-[(4*R*)-(4-ethyl-Δ²-1,3-oxazolin-2-yl)-2-(4*S*)-(4-ethyl-Δ²-1,3-oxazolin-2-yl)]benzene-*N,N*}palladium(II) hexafluorophosphate, (*R,S*)-1A. 0.048 g of [Pd(η³-C₃H₅)(μ-Cl)]₂ (0.13 mmol) and 0.061 g of (*R,S*)-**A** (0.22 mmol) were dissolved

in 20 cm³ of absolute ethanol. The mixture was stirred at room temperature for 30 min. 0.030 g of NH$_4$PF$_6$ (0.16 mmol) was then added and the mixture stirred for 18 h at room temperature. The solvent was removed under reduced pressure, affording an oil which was dissolved in 25 cm³ of dichloromethane. The mixture was extracted with water (3 × 15 cm³) until neutral pH. The organic phase was dried over anhydrous Na$_2$SO$_4$, filtered, and the solvent removed under reduced pressure. After addition of diethyl ether a white solid was obtained. The product was dried under reduced pressure. Yield: 0.093 g (81%). IR(KBr): 1651 (st, C=N), 842 cm^{-1} (st, P–F). Calc. for C$_{19}$H$_{25}$F$_6$N$_2$O$_2$PPd: C, 40.41; H, 4.46; N, 4.96%. Found: C, 40.48; H, 4.62; N, 4.00%. Melting point: 175 °C. MS (FAB positive): *m/z* 421 ([M − PF$_6$]$^+$).

The compounds **1B**–**1D** were synthesized in a similar way.

(η³-Allyl){1,2-bis[(4S)-(4-isopropyl-Δ²-1,3-oxazolin-2-yl)]-benzene-*N*,*N*}palladium(II) hexafluorophosphate, (S,S)-1B. Starting materials: 0.367 g (1.00 mmol) of [Pd(η³-C$_3$H$_5$)(μ-Cl)]$_2$, 0.345 g (1.15 mmol) of (S,S)-**B**, and 0.134 g (0.82 mmol) of NH$_4$PF$_6$. Yield: 0.640 g (98%). IR(KBr): 1653 (st, C=N), 837 cm^{-1} (st, P–F). Calc. for C$_{21}$H$_{29}$F$_6$N$_2$O$_2$PPd: C, 42.54; H, 4.93; N, 4.73%. Found: C, 41.53; H, 5.00; N, 4.95%. Melting point: 187 °C. MS (FAB positive): *m/z* 448 ([M − PF$_6$]$^+$).

(η³-Allyl){1,2-bis[(4S)-(4-ethyl-Δ²-1,3-oxazolin-2-yl)]ethane-*N*,*N*}palladium(II) hexafluorophosphate, (R,R)-1C. Starting materials: 0.133 g (0.29 mmol) of [Pd(η³-C$_3$H$_5$)(μ-Br)]$_2$, 0.132 g (6 mmol) of (R,R)-**C**, and 0.87 g (0.14 mmol) of NH$_4$PF$_6$. Yield: 0.130 g (85.5%). IR(KBr): 1664 and 1648 (st, C=N), 838 cm^{-1} (st, P–F). Calc. for C$_{15}$H$_{25}$F$_6$N$_2$O$_2$PPd: C, 34.86; H, 4.84; N, 5.42%. Found: C, 34.57; H, 4.80; N, 5.41%. Melting point: 191 °C. MS (FAB positive): *m/z* 371 ([M − PF$_6$]$^+$).

(η³-Allyl){1,2-bis[(4S)-(4-isopropyl-Δ²-1,3-oxazolin-2-yl)]-ethane-*N*,*N*}palladium(II) hexafluorophosphate, (S,S)-1D. Starting materials: 0.133 g (0.29 mmol) of [Pd(η³-C$_3$H$_5$)(μ-Br)]$_2$, 0.148 g (0.6 mmol) of (R,R)-**C**, and 0.87 g (0.14 mmol) of NH$_4$PF$_6$. Yield: 0.290 g (91%). IR(KBr): 1671 and 1650 (st, C=N), 839 cm^{-1} (st, P–F). Calc. for C$_{17}$H$_{29}$F$_6$N$_2$O$_2$PPd: C, 37.47; H, 5.32; N, 5.14%. Found: C, 37.42; H, 5.31 ; N, 5.13%. Melting point: 195 °C (decomposition). MS (FAB positive): *m/z* 399 ([M − PF$_6$]$^+$).

{1,2-Bis[(4R)-(4-ethyl-Δ²-1,3-oxazolin-2-yl)]benzene-*N*,*N*}-(η³-1,3-diphenylallyl)palladium(II) hexafluorophosphate, (R,R)-2A. 0.076 g of [Pd(η³-1,3-Ph$_2$C$_3$H$_3$)(μ-Cl)]$_2$ (0.11 mmol) and 0.065 g of (R,R)-**A** (0.24 mmol) were dissolved in 20 cm³ of a mixture of dichloromethane, chloroform, absolute ethanol and methanol, using the same volume of each (5 cm³). The mixture was stirred at room temperature for 30 min. 0.120 g of NH$_4$PF$_6$ (0.72 mmol) was then added and the mixture stirred for three days at room temperature. The solvent was removed under reduced pressure, affording an oil, which was dissolved in 25 cm³ of dichloromethane–chloroform (1 : 1). The mixture was extracted with water (3 × 10 cm³), until neutral pH. The organic phase was dried over anhydrous Na$_2$SO$_4$, filtered, and the solvent removed under reduced pressure. After addition of diethyl ether a yellow solid was obtained. The product was dried under reduced pressure. Yield: 0.076 g (88%). IR(KBr): 1651 (st, C=N), 842 cm^{-1} (st, P–F). Calc. for C$_{31}$H$_{33}$F$_6$N$_2$O$_2$PPd·0.5Et$_2$O: C, 52.91; H, 5.00; N, 3.71%. Found: C, 52.41; H, 5.00; N, 3.90%. Melting point (decomposition): 220 °C. MS (FAB positive): *m/z* 572 ([M − PF$_6$]$^+$).

The following compounds were synthesized in a similar way.

(η³-1,3-Diphenylallyl){1-[(4R)-(4-ethyl-Δ²-1,3-oxazolin-2-yl)-2-(4S)-(4-ethyl-Δ²-1,3-oxazolin-2-yl)]benzene-*N*,*N*}palladium(II) hexafluorophosphate, (R,S)-2A. Starting materials: 0.113 g (0.17 mmol) of [Pd(η³-1,3-Ph$_2$C$_3$H$_3$)(μ-Cl)]$_2$, 0.100 g (0.35 mmol) of

(R,S)-**A**, and 0.173 g (1.06 mmol) of NH$_4$PF$_6$. Yield: 0.107 g (89%). IR(KBr): 1658 (st, C=N), 839 cm^{-1} (st, P–F). Melting point (decomposition): 225 °C. MS (FAB positive): *m/z* 572 ([M − PF$_6$]$^+$).

{1,2-Bis[(4S)-(4-isopropyl-Δ²-1,3-oxazolin-2-yl)]benzene-*N*,*N*}(η³-1,3-diphenylallyl)palladium(II) hexafluorophosphate, (S,S)-2B. Starting materials: 0.081 g (0.12 mmol) of [Pd(η³-1,3-Ph$_2$C$_3$H$_3$)(μ-Cl)]$_2$, 0.076 g (0.25 mmol) of (S,S)-**B**, and 0.060 g (0.36 mmol) of NH$_4$PF$_6$. Yield: 0.177 g (98%). IR(KBr): 1648 (st, C=N), 845 cm^{-1} (st, P–F). Calc. for C$_{33}$H$_{37}$F$_6$N$_2$O$_2$PPd: C, 53.20; H, 5.00; N, 3.76%. Found: C, 53.32; H, 4.90; N, 3.74%. MS (FAB positive): *m/z* 601 ([M − PF$_6$]$^+$).

Crystallography

The crystallographic data are summarized in Table 4. Orange crystals of [Ni((R,S)-**A**)$_2$][ClO$_4$]$_2$ were obtained by slow evaporation of an acetonitrile solution of complex, colorless crystals of (S,S)-**1B** and yellow crystals of (R,S)-**2A** obtained by slow diffusion of hexane over a chloroform–dichloromethane solution of the complexes. The latter complex crystallizes with two molecules of solvent, one of chloroform and one of dichloromethane. Yellow crystals of (S,S)-**2B** and colorless crystals of (R,S)-**1A** were obtained by slow diffusion of hexane over a chloroform–dichloromethane solution of the complex, colorless crystals of (S,S)-**1D** by slow diffusion of hexane and diethyl ether over a chloroform–dichloromethane solution of the complex.

The crystal data for [Ni((R,S)-**A**)$_2$][ClO$_4$]$_2$ and (R,S)-**1A** were measured on an Enraf-Nonius CAD4 four-circle diffractometer. Unit-cell parameters were determined from automatic centering of 25 reflections (12 < θ < 21°) and were refined by the least-squares method on F^2. Intensities were collected with graphite monochromatized Mo-Kα radiation (λ = 0.71069 Å), using the ω–2θ scan technique. Three reflections were measured every two hours as orientation and intensity controls, and significant intensity decay was not observed. Lorentz-polarization but not absorption corrections were made. The structure was solved by direct methods, using the SHELXS 97 computer program,[15] and refined by full-matrix least squares with SHELXL 97.[16] Values of f, f', and f'' were taken from ref. 17. The extinction coefficient was 0.0120(14).[18] All hydrogen atoms were computed and refined with an overall isotropic thermal parameter.

The crystal data for (R,S)-**2A**, (S,S)-**1B**, (S,S)-**2B**, and (S,S)-**1D** were collected using a Bruker SMART CCD-based diffractometer. Intensities were collected as above. Cell parameters were retrieved using SMART software[19] and refined using SAINT[20] on all observed reflections. Data reduction was performed using the SAINT software. Absorption corrections used SADABS.[21] The structures were solved and refined as above. The extinction coefficient was −0.02(3) for (S,S)-**1B**, 0.00(2) for (S,S)–**2B** and 0.04(3) for (S,S)-**1D**. All non-hydrogen atoms were refined anisotropically. Hydrogen atoms were included in calculated positions and refined as a riding model.

CCDC reference numbers 160662–160666 and 161470.

See http://www.rsc.org/suppdata/dt/b0/b007743g/ for crystallographic data in CIF or other electronic format.

General procedure for palladium-catalyzed allylic alkylation

The precursor (0.02 mmol of complex of type **1**) was dissolved in 2 cm³ of CH$_2$Cl$_2$. *rac*-1,3-Diphenyl-2-propenyl acetate (252 mg, 1 mmol), dissolved in 2 cm³ of CH$_2$Cl$_2$, was added, followed by dimethyl malonate (396 mg, 3 mmol), BSA [*N*,*O*-bis(trimethylsilyl)acetamide] (610 mg, 3 mmol), and a catalytic amount of KOAc. The mixture was stirred at room temperature until the substrate had been consumed (unless stated otherwise), monitored by TLC (eluent: hexane–ethyl acetate, 4 : 1).

Table 4 Crystal data for complexes [Ni((R,S)-A)₂][ClO₄]₂, (R,S)-**1A**, (R,S)-**2A**, (S,S)-**1B**, (S,S)-**2B**, and (S,S)-**1D**

	[Ni((R,S)-A)₂][ClO₄]₂	(R,S)-**1A**	(R,S)-**2A**	(S,S)-**1B**	(S,S)-**2B**	(S,S)-**1D**
Formula	$C_{32}H_{40}Cl_2N_4O_{12}Ni$	$C_{19}H_{25}F_6N_2O_2\cdot PPd$	$C_{33}H_{36}Cl_5F_6N_2O_2\cdot PPd$	$C_{21}H_{29}F_6N_2O_2\cdot PPd$	$C_{33}H_{37}F_6N_2O_2\cdot PPd$	$C_{17}H_{29}F_6N_2O_2\cdot PPd$
Molecular weight	802.29	567.80	921.26	592.83	745.02	544.79
T/K	293(2)	293(2)	298(2)	298(2)	298(2)	298(2)
Crystal system	Monoclinic	Orthorhombic	Monoclinic	Orthorhombic	Monoclinic	Triclinic
Space group	$P2_1/n$	$Pbca$	$P2_1/c$	$P2_12_12_1$	$P2_1$	$P1$
a/Å	9.992(5)	16.304(9)	14.061(3)	11.470(2)	9.3654(2)	8.4737(2)
b/Å	17.166(2)	16.589(3)	11.9323(15)	13.530(2)	16.3689(2)	8.9915(3)
c/Å	10.642(4)	17.088()	22.782(3)	16.332(3)	10.9488(2)	9.2028(2)
a/°						81.2790(10)
β/°	91.01(4)		95.939(9)		93.2020(10)	62.7870(10)
γ/°						66.1180(10)
V/Å³	1825.1(12)	4622(3)	3801.8(11)	2534.6(8)	1675.84(5)	569.69(3)
Z	2	8	4	4	2	1
μ/mm⁻¹	0.669	0.938	0.944	0.859	0.667	0.947
Reflections collected	5585	6721	20800	14123	9339	4026
Independent reflections	5304	6677	9287	6280	5836	3234
	[R_{int} = 0.0262]	[R_{int} = 0.0292]	[R_{int} = 0.0297]	[R_{int} = 0.0289]	[R_{int} = 0.0185]	[R_{int} = 0.0167]
Final $R1$, $wR2$ indices [$I > 2\sigma(I)$]	0.0431, 0.1200	0.0354, 0.0908	0.0607, 0.1633	0.0375, 0.0867	0.0304, 0.0646	0.0315, 0.0810
(all data)	0.0570, 0.1285	0.1129, 0.1173	0.0908, 0.1864	0.0483, 0.0929	0.0377, 0.0682	0.0321, 0.0818

Then the solution was diluted with diethyl ether, filtered over Celite, and washed successively with an aqueous solution of ammonium chloride (10%) and water (2 × 10 cm³). The organic phase was dried over anhydrous Na₂SO₄, filtered, and solvent removed under reduced pressure. The product was purified by column chromatography (SiO₂; ethyl acetate), followed by heating at 130 °C under vacuum. The enantiomeric excesses were determined by HPLC on a Chiralcel OD column, using hexane–*i*PrOH, 99 : 1, as eluent, in a flow of 0.3 cm³ min⁻¹ and pressure 10 bar.

Acknowledgements

References

1 A. K. Ghosh, P. Mathivanan and J. Cappiello, *Tetrahedron*: *Asymmetry*, 1998, **9**, 1 and references therein; A. Pfaltz, *Adv. Catal. Processes*, 1995, **1**, 61 and references therein; A. Pfaltz, *Acc. Chem. Res.*, 1993, **26**, 339.

2 (*a*) D. Müller, G. Umbricht, B. Weber and A. Pfaltz, *Helv. Chim. Acta*, 1991, **74**, 232; (*b*) U. Leutenegger, G. Umbricht, C. Fahrni, P. von Matt and A. Pfaltz, *Tetrahedron*, 1992, **48**, 2143; (*c*) P. von Matt, G. C. Lloyd-Jones, A. B. E. Minidis, A. Pfaltz, L. Macko, M. Neuburger, M. Zehnder, H. Rüegger and P. S. Pregosin, *Helv. Chim. Acta*, 1995, **78**, 265; (*d*) O. Hoarau, H. Aït-Haddou, M. Castro and G. A. Balavoine, *Tetrahedron*: *Asymmetry*, 1997, **8**, 3755.

3 G. Helmchen, *J. Organomet. Chem.*, 1999, **576**, 203 and references therein.

4 M. Zender, M. Neuburger, P. von Matt and A. Pfaltz, *Acta Crystallogr.*, *Sect. C*, 1995, **51**, 1109; O. Hoarau, H. Aït-Haddou,

J.-C. Daran, D. Cramaïlère and G. G. A. Balavoine, *Organometallics*, 1999, **18**, 4718.

5 (*a*) C. Bolm, K. Weickhardt, M. Zehnder and T. Ranff, *Chem. Ber.*, 1991, **124**, 1173; (*b*) C. Bolm, *Angew. Chem.*, *Int. Ed. Engl.*, 1991, **30**, 542.

6 A. V. Bedekar, E. B. Koroleva and P. G.Andersson, *J. Org. Chem.*, 1997, **62**, 4229; A. J. Davenport, D. L. Davies, J. Fawcett, S. A. Garratt, L. Lad and D. R. Russell, *Chem. Commun.*, 1997, 2347; I. W. Davies, C. H. Senannayake, R. D. Larsen, T. R. Verhoeven and P. J. Reider, *Tetrahedron Lett.*, 1996, **37**, 1725; Y. Takemoto, S. Kuraoka, N. Hamaue, K. Aoe, H. Hiramatsu and C. Iwata, *Tetrahedron*, 1996, **52**, 14177.

7 (*a*) For ligand **A**: A. El Hatimi, M. Gómez, S. Jansat, G. Muller, M. Font-Bardía and X. Solans, *J. Chem. Soc.*, *Dalton Trans.*, 1998, 4229 and references therein; (*b*) For ligands **B** and **D**, see reference 5(*a*).

8 N. Baltzer, L. Macko, S. Schaffner and M. Zehnder, *Helv. Chim. Acta*, 1996, **79**, 803.

9 J. L. Led and H. Gesmar, *J. Magn. Reson.*, 1982, **49**, 444.

10 B. M. Trost and D. J. Murphy, *Organometallics*, 1985, **4**, 1143.

11 U. Leutenegger, G. Umbricht, C. Fahrni, P. V. Matt and A. Pfaltz, *Tetrahedron*, 1992, **48**, 2143.

12 D. D. Perrin, W. L. F. Armarego and D. R. Perrin, in *Purification of Laboratory Chemicals*, Pergamon Press, Oxford, 3rd edn., 1988.

13 M. J. McKennon, A. I. Meyers, K. Drauz and M. Schwarm, *J. Org. Chem.*, 1993, **58**, 3568.

14 Y. Tatsuno, T. Yoshida and S. Otsuka, *Inorg. Synth.*, 1990, **28**, 342.

15 G. M. Sheldrick. SHELXS 97, a computer program for crystal structure determination, University of Göttingen, 1997.

16 G. M Sheldrick. SHELXL 97, a computer program for crystal structure refinement, University of Göttingen, 1997.

17 *International Tables for X-Ray Crystallography*, Kynoch Press, Birmingham, 1974, vol. IV, pp. 99, 100 and 149.

18 H. D. Flack, *Acta Crystallogr.*, *Sect. A*, 1983, **39**, 876.

19 SMART, V. 4.210, Bruker Analytical X-ray Systems, Madison, WI, 1995.

20 SAINT, V. 4.050, Bruker Analytical X-ray Systems, Madison, WI, 1995.

21 Program for absorption corrections using the Bruker CCD based on the method of R. H. Blessing, *Acta Crystallogr.*, *Sect. A*, 1995, **51**, 33.